

RELATIONSHIP OF MAGNETISM AND  
SUPERCONDUCTIVITY IN HEAVY-FERMION  
SYSTEMS: PRESSURE STUDIES ON  $\text{CeMIn}_5$   
AND  $\text{Ce}_2\text{MIn}_8$  ( $\text{M} = \text{Co}, \text{Rh}, \text{Ir}$ )\*

M. NICKLAS<sup>a</sup>, V.A. SIDOROV<sup>a,b</sup>, H.A. BORGES<sup>a,c</sup>, N.O. MORENO<sup>a</sup>  
P.G. PAGLIUSO<sup>a</sup>, J.L. SARRAO<sup>a</sup>, AND J.D. THOMPSON<sup>a</sup>

<sup>a</sup>Los Alamos National Laboratory, Los Alamos, NM 87545, USA

<sup>b</sup>Institute for High Pressure Physics, Russian Academy of Sciences  
Troitsk, Russia

<sup>c</sup>Departamento de Física, Pontifícia Universidade Católica do Rio de Janeiro  
Rio de Janeiro, Brazil

*(Received July 10, 2002)*

We report studies of the pressure-dependent superconducting and Néel temperatures of the heavy fermion compound  $\text{Ce}_2\text{RhIn}_8$  and the doping series  $\text{CeRh}_{1-x}\text{Ir}_x\text{In}_5$ . Systematic evolution of their groundstates with pressure emphasizes the importance of spin fluctuations for superconductivity.

PACS numbers: 74.70.Tx, 62.50.+p, 73.43.Nq, 71.27.+a

## 1. Introduction

The relationship between magnetism and superconductivity is a recurring theme of heavy fermion physics, exemplified by  $\text{CeIn}_3$ , which is an ambient pressure antiferromagnet, showing superconductivity under hydrostatic pressure as magnetism is suppressed [1]. The family of  $\text{CeMIn}_5$  and  $\text{Ce}_2\text{MIn}_8$  ( $\text{M} = \text{Co}, \text{Rh}, \text{Ir}$ ) is closely related to  $\text{CeIn}_3$ , derived from the  $\text{CeIn}_3$  structure by inserting, respectively, one or two  $\text{CeIn}_3$  layers between a single  $\text{MIn}_2$  layer. Antiferromagnetism and superconductivity are found in these systems. A feature of these compounds is their remarkably high ( $>2\text{K}$ ) superconducting temperature compared to other heavy fermion superconductors and  $\text{CeIn}_3$  ( $T_c \approx 200 \text{ mK}$ ) in particular. Hydrostatic pressure and doping allow an investigation of the relationship of superconductivity and antiferromagnetism as a function of external parameters.

---

\* Presented at the International Conference on Strongly Correlated Electron Systems, (SCES 02), Cracow, Poland, July 10–13, 2002.

CeIn<sub>3</sub>, CeRhIn<sub>5</sub>, and Ce<sub>2</sub>RhIn<sub>8</sub> are ambient pressure antiferromagnets with  $T_N = 10$  K, 3.8 K and 2.8 K [1–3], respectively. CeIn<sub>3</sub> and CeRhIn<sub>5</sub> become superconducting at hydrostatic pressures of 25 kbar and 16 kbar, respectively, but CeRhIn<sub>5</sub> with an order of magnitude higher  $T_c$ , 2.1 K compared to CeIn<sub>3</sub> [1, 2]. In this study we present results for Ce<sub>2</sub>RhIn<sub>8</sub>, which is, from a structural point of view, closer to CeRhIn<sub>5</sub>, whereas its magnetic structure is similar to CeIn<sub>3</sub> [4, 5].

CeRh<sub>1-x</sub>Ir<sub>x</sub>In<sub>5</sub> shows a rich phase diagram: for  $x < 0.3$  the groundstate is antiferromagnetic; magnetism and superconductivity coexist for an intermediate range of  $x$  and unusual superconductivity appears at large  $x$  [6]. CeIrIn<sub>5</sub> has a zero-resistance transition at about 1.2 K, but bulk superconductivity, confirmed by susceptibility and specific heat measurements, is established at only 400 mK [7–9]. We study the pressure-temperature phase diagram for representative compounds in this doping series and compare our results with the  $x$ - $T$  phase diagram [6]. We present detailed results for CeRh<sub>0.9</sub>Ir<sub>0.1</sub>In<sub>5</sub> and CeRh<sub>0.25</sub>Ir<sub>0.75</sub>In<sub>5</sub>, as representative of the alloy series. The first is an ambient pressure antiferromagnet, whereas the latter is superconducting at low temperatures.

## 2. Experimental results

CeRh<sub>1-x</sub>Ir<sub>x</sub>In<sub>5</sub> and Ce<sub>2</sub>RhIn<sub>8</sub> single crystals were grown out of excess In-flux. X-ray diffraction on powdered crystals revealed single-phase material. The samples were carefully screened by electrical resistance and susceptibility measurements for free In that might be present in the crystals. Only samples without any detectable (less than 0.01 vol%) free indium were used for the present pressure studies. Measurements of the dc and ac susceptibility were performed in a Quantum Design SQUID and a homemade coil system, respectively. Resistance measurements were carried out by a standard four-probe ac-technique using a resistance bridge, where the current was applied in the ( $a, b$ )-plane of the samples. Three clamp-type cells with Flourinert-75 serving as pressure medium were used to generate various fixed hydrostatic pressures up to 6 kbar for SQUID and 17 or 23 kbar for resistivity measurements. In addition, Ce<sub>2</sub>RhIn<sub>8</sub> was studied at hydrostatic pressures to 50 kbar produced in a toroidal anvil cell using a glycerol-water mixture (3:2, volume ratio). In both types of cells, the superconducting transition of Pb (Sn), which served as a pressure gauge, remained sharp at all pressures, indicating a pressure gradient of less than 1–2% of the applied pressure.

2.1.  $CeRh_{1-x}Ir_xIn_5$ 

The  $a$  lattice constant, which is the nearest-neighbor Ce-Ce spacing in the  $CeRh_{1-x}Ir_xIn_5$  series structure, expands from  $a = 4.652 \text{ \AA}$  for  $CeRhIn_5$  to  $a = 4.668 \text{ \AA}$  for  $CeIrIn_5$ . In contrast, the  $c$  axis shrinks from  $c = 7.542 \text{ \AA}$  to  $c = 7.515 \text{ \AA}$  [10]. This corresponds to a cell volume increase of 0.3% from  $CeRhIn_5$  to  $CeIrIn_5$ . We estimate an uncertainty in  $x$  of  $\pm 0.05$  at a given composition, this variation is consistent with independent crystal-to-crystal variations in ground-state properties. However, the value of  $x$  in a given crystal is always well defined; we observe no evidence for concentration inhomogeneity or phase segregation as judged by the sharpness of diffraction peaks that are observed across the series.

Figure 1 shows the low temperature resistivity of  $CeRh_{0.9}Ir_{0.1}In_5$  for different applied hydrostatic pressures. The change in curvature reflects the Néel transition in the resistivity, which has been confirmed by dc-susceptibility and specific heat measurements at ambient pressure. Increasing pressure is accompanied by an increasing residual resistivity  $\rho_0$  as in  $CeRhIn_5$  [2]. The Néel temperature  $T_N$  at applied pressures is derived from the temperature at which there is a maximum in  $\partial\rho/\partial T$ .  $T_N(P)$  initially increases with pressure with an estimated slope of  $\partial T_N/\partial P \approx 53 \text{ mK/kbar}$  similar to  $CeRhIn_5$  ( $\partial T_N/\partial P \approx 9 \text{ mK/kbar}$ ) [2] as shown in Fig. 2.  $T_N$  shows a maximum at about 5 kbar ( $T_N \approx 4.95 \text{ K}$ ) and with further increasing pressure shifts to lower temperatures. The feature in resistivity

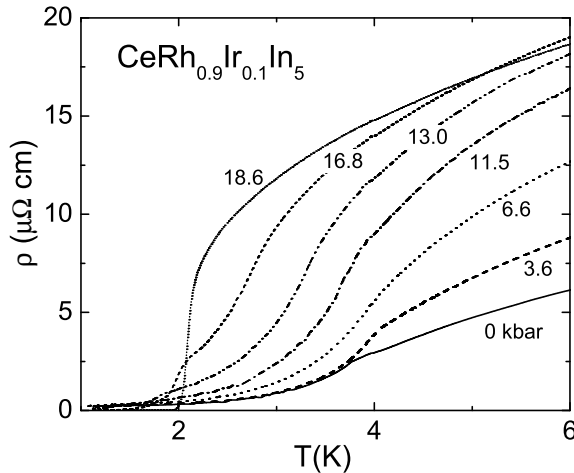


Fig. 1. Low temperature resistivity  $\rho$  for  $CeRh_{0.9}Ir_{0.1}In_5$  plotted for different hydrostatic pressures. The change in curvature indicates the Néel transition  $T_N$  that is observed for pressures up to 16.8 kbar.

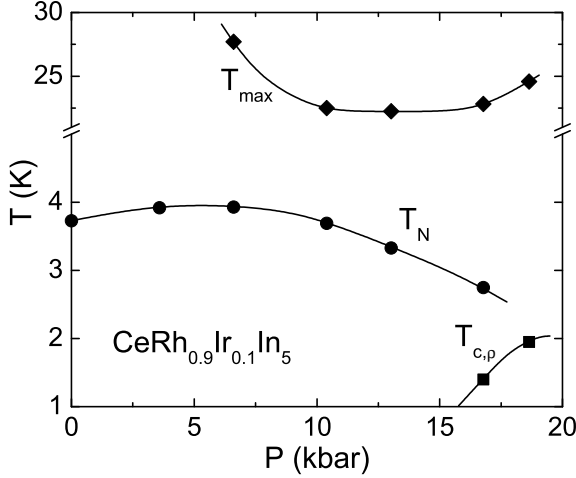


Fig. 2.  $T$ - $P$  phase diagram of  $\text{CeRh}_{0.9}\text{Ir}_{0.1}\text{In}_5$ . The Néel temperature  $T_N$  is suppressed with increasing pressure. A zero-resistance state below  $T_{c,\rho}$  appears above 16.8 kbar.  $T_{\text{max}}$  shows a broad minimum. The lines are to guide the eyes.

indicating magnetic order is still observable at 16.8 kbar, where we also find a zero resistance state below 1.40 K. The superconducting transition sharpens and moves to higher temperatures ( $T_c = 1.95$  K) at 18.6 kbar, where no indication of a magnetic transition is observable. (The  $T$ - $P$  phase diagram is plotted in Fig. 2.)

There is no maximum in  $\rho(T)$  for pressures below 5 kbar, but one appears first at  $P = 6.6$  kbar at  $T_{\text{max}} = 27.7$  K.  $T_{\text{max}}$  initially decreases to 22.5 K at 10.4 kbar, shows a broad minimum and increases at higher pressures. This behavior summarized in Fig. 2 is very similar to the response of undoped  $\text{CeRhIn}_5$  [2] and seems not to be affected by light Ir-doping.

$\text{CeRh}_{0.25}\text{Ir}_{0.75}\text{In}_5$ , on the Ir-rich side of the  $T$ - $x$  phase diagram, is superconducting at ambient pressure. Zero-resistivity appears below  $T_{c,\rho} = 965$  mK, without any detectable feature in ac susceptibility. The bulk transition takes place at a much lower temperature, as shown in Fig. 3 where a complete Meissner effect develops below  $T_{c,\chi_{\text{final}}} \approx 560$  mK. A similar discrepancy exists between  $T_{c,\rho}$  and  $T_{c,\chi}$  in  $\text{CeIrIn}_5$  [11].

The response of the resistivity to hydrostatic pressure is shown in figure 4 for 0, 5.1, 10.1 and 14.7 kbar. At ambient pressure the resistivity reaches a maximum at 37.7 K that generally is associated with a crossover from incoherent Kondo-like scattering at high temperatures to a heavy-fermion band state at low temperatures. The temperature of the maximum,  $T_{\text{max}}$ , is a linear function of pressure  $P$  with  $dT_{\text{max}}/dP = 2.3$  K/kbar, which is

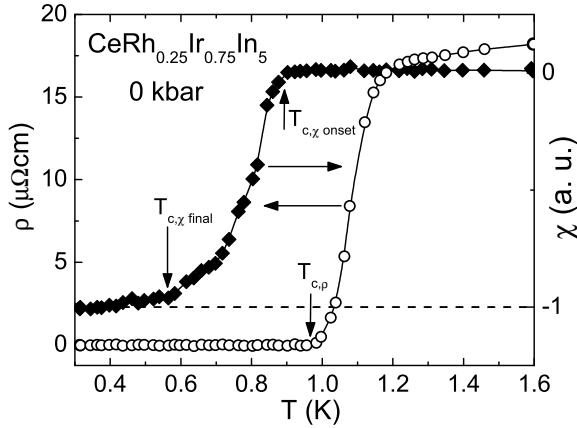


Fig. 3. Resistivity  $\rho$  and ac susceptibility  $\chi$  of  $\text{CeRh}_{0.25}\text{Ir}_{0.75}\text{In}_5$  at ambient pressure. Bulk superconductivity is observed well below the zero-resistance transition.

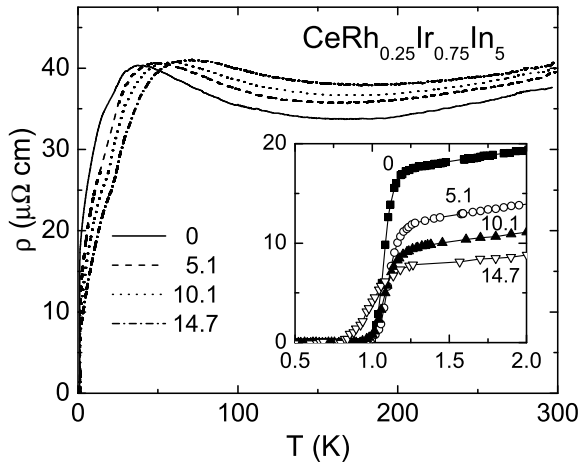


Fig. 4. Resistivity  $\rho$  of  $\text{CeRh}_{0.25}\text{Ir}_{0.75}\text{In}_5$  for different hydrostatic pressures. The inset shows the zero-resistance transition.

close to what is found for the isoelectronic superconductor  $\text{CeCoIn}_5$  with  $dT_{\text{max}}/dP = 2.8$  K/kbar [12]. The resistivity above  $T_{\text{max}}$  increases monotonically, whereas, the resistivity below  $T_{\text{max}}$  decreases. This is a typical behavior for Ce-based heavy fermion compounds [14]. A detailed view of the low temperature part is given in the inset of figure 4. The resistivity just above the superconducting transition loses more than half of its value at 14.7 kbar compared to its ambient pressure value.

With increasing pressure the resistive, as well as the bulk, transition temperatures decrease after a nearly constant pressure dependence at low pressures (see Fig. 5). The width of the resistive transition increases linearly over the whole pressure range by nearly a factor of two ( $\Delta T_{c,\rho} = 175$  mK at ambient pressure,  $\Delta T_{c,\rho} = 320$  mK at 17 kbar). Similar behavior is observed in related compounds of the  $\text{CeMIn}_5$  and  $\text{Ce}_2\text{MIn}_8$  ( $M = \text{Co}, \text{Rh}, \text{Ir}$ ) family. In  $\text{CeCoIn}_5$ , for example, increasing  $T_c$  below 16 kbar is accompanied by a sharpening of the resistive transition, while the transition broadens again with decreasing  $T_c$  at higher pressures [12, 15, 16]. The sharpest transition is always found at the highest  $T_c$ . The onset of diamagnetism behaves like the  $T_{c,\rho}(P)$ , remaining constant to 6 kbar but decreasing at higher  $P$ . In contrast to the onset temperature,  $T_{c,\chi_{\text{final}}}$  starts to decrease for  $P \gtrsim 3$  kbar.

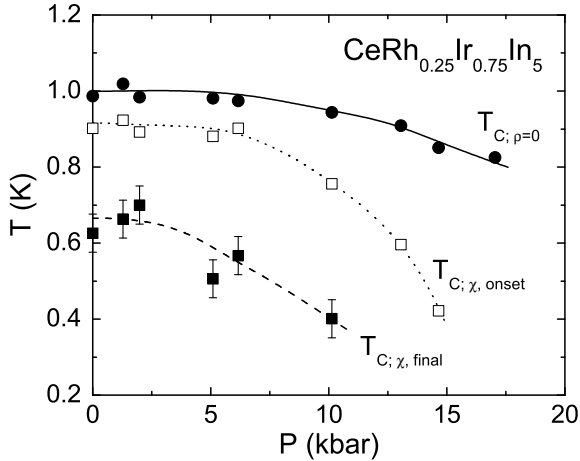


Fig. 5. Pressure-temperature phase diagram of  $\text{CeRh}_{0.25}\text{Ir}_{0.75}\text{In}_5$ . Plotted are the zero-resistance transition  $T_{c;\rho=0}$  and the onset  $T_{c,\chi_{\text{onset}}}$  and the temperature  $T_{c,\chi_{\text{final}}}$  of the completed bulk transition obtained from susceptibility measurements. The lines are to guide the eyes.

At atmospheric pressure, the discrepancy between the resistive transition  $T_{c,\rho}$  and the bulk superconducting transition  $T_{c,\text{bulk}}$  in  $\text{CeRh}_{1-x}\text{Ir}_x\text{In}_5$  is greatest near  $x \approx 0.9$  [6, 7] and vanishes with decreasing Ir-concentration, approaching zero separation at  $\text{CeRh}_{0.5}\text{Ir}_{0.5}\text{In}_5$  [6]. We have found that the difference between  $T_{c,\rho}$  and  $T_{c,\text{bulk}}$  decreases with applied pressure in  $\text{CeIrIn}_5$  and finally vanishes at about 20 kbar and, further, that  $T_{c,\rho}$  and  $T_{c,\text{bulk}}$  coincide for  $0 < x < 0.5$  at ambient and high pressure [18]. This behavior is in contrast to the increasing difference between  $T_{c,\rho}$  and  $T_{c,\text{bulk}}$  with pressure in  $\text{CeRh}_{0.25}\text{Ir}_{0.75}\text{In}_5$  (see figure 5). Specific heat, susceptibility

and resistivity measurements at  $P = 0$  on samples  $x \geq 0.5$  suggest that the inhomogeneous superconductivity is intrinsic and due to strain introduced by crystallographic defects [9]. However, the pressure dependence of  $T_{c,\rho}$  and  $T_{c,\text{bulk}}$  we find suggest that either the defects have an unusual pressure response or that additional mechanisms may be responsible for this behavior.

The doping-temperature phase diagram of  $\text{CeRh}_{1-x}\text{Ir}_x\text{In}_5$  in figure 6 summarizes the effect of pressure on the antiferromagnetism and superconductivity. At ambient pressure antiferromagnetism persists for  $0 \leq x \leq 0.6$ . The Néel temperature stays constant for  $x \lesssim 0.4$ , but vanishes rather abruptly with further increasing Ir-concentration at  $x_c \approx 0.6$  [6]. Superconductivity is observed over a broad range of doping,  $0.3 \leq x < 1$ . The coexistence of magnetism and superconductivity in concentration range  $0.3 \leq x \leq 0.6$  [6] is also confirmed microscopically by NMR measurements [17].

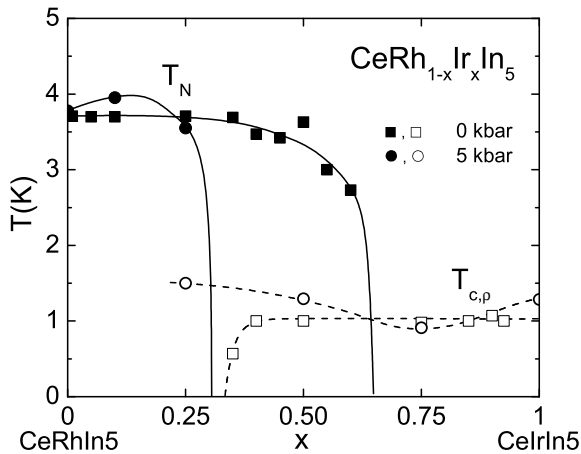


Fig. 6. Phase diagram for the doping series  $\text{CeRh}_{1-x}\text{Ir}_x\text{In}_5$  at ambient pressure [6] and at 5 kbar. The data at 5 kbar is interpolated from the actually measured data for the concerning concentration. The lines are to guide the eyes.

For comparison 5 kbar data for  $T_N$  and  $T_{c,\rho}$ , interpolated from the corresponding pressure-temperature phase diagrams are included in Fig. 6. The critical concentration for the suppression of antiferromagnetism to zero temperature  $x_c$  shifts from  $x_c(P = 0) \approx 0.6$  to  $x_c(P = 5\text{kbar}) \approx 0.3$ . This is accompanied by an increase of  $T_N$  for  $x = 0.1$  leading to a maximum in  $T_N(x)$ . Superconductivity exists in an extended concentration range from  $x = 0.25$  to 1, where now superconductivity coexists with magnetism in  $\text{CeRh}_{0.75}\text{Ir}_{0.25}\text{In}_5$ . The superconducting transition temperature has increased for all concentrations except  $x = 0.75$ , resulting in the development of a minimum in  $T_{c,\rho}$  around  $x = 0.75$ .

In CeRhIn<sub>5</sub>, the susceptibility reveals a maximum at about  $T_{\chi,M} = 7.5$  K, [2] where inelastic neutron scattering finds the development of antiferromagnetic spin correlations in the CeIn<sub>3</sub>-layers [13]. Applied pressure suppresses  $T_{\chi,M}$ , which extrapolates to zero at a pressure required to induce superconductivity. This pressure-induced decrease in  $T_{\chi,M}$  is accompanied by a large increase in the residual resistivity, which can be understood if there is a corresponding increase in scattering from antiferromagnetic spin fluctuations [2]. Measurements of the susceptibility for field applied along the *c* axis,  $\chi_c$ , and along the *a* axis,  $\chi_a$ , in the doping series [6] reveal characteristic evolution of each component. While the maximum in  $\chi_c(T)$  disappears near the concentration at which superconductivity is first observed, the maximum in  $\chi_a(T)$  is lost around  $x \approx 0.6$ , where magnetic order is suppressed. The disappearance of the maximum in the susceptibility is accompanied by a characteristic change of the pressure dependence of  $\rho_0(P)$ . The residual resistivity  $\rho_0$  increases with pressure for Ir-concentrations  $x < 0.5$  ( $\partial\rho_0/\partial P > 0$ ). Though we have not determined  $T_{\chi,M}(P)$  for these alloys, we believe that the positive  $\partial\rho_0/\partial P$  arises from the same mechanism as in CeRhIn<sub>5</sub> and this leads to a higher maximum  $T_c(P)$  in this part of the phase diagram. For  $x \geq 0.5$ ,  $\partial\rho_0/\partial P$  is negative, implying a shift of the spin fluctuation spectrum to higher energies, which might account for a lower maximum  $T_c(P)$  in this region of the phase diagram.

## 2.2. Ce<sub>2</sub>RhIn<sub>8</sub>

At ambient pressure Ce<sub>2</sub>RhIn<sub>8</sub> orders antiferromagnetically with a Néel-temperature  $T_N = 2.8$  K below which the magnetic structure is commensurate and similar to CeIn<sub>3</sub> [5]. In contrast, CeRhIn<sub>5</sub> has an incommensurate magnetic structure below its Néel-temperature  $T_N = 3.8$  K. A second magnetic transition to an incommensurate state at lower temperatures  $T_{LN} = 1.65$  also is found in Ce<sub>2</sub>RhIn<sub>8</sub> [19]. In the following, we discuss the pressure-temperature phase diagram of Ce<sub>2</sub>RhIn<sub>8</sub> and compare it to the phase diagram of CeIn<sub>3</sub>, CeRhIn<sub>5</sub> and the doping series CeRh<sub>1-x</sub>Ir<sub>x</sub>In<sub>5</sub>. A complete study of the high pressure properties of Ce<sub>2</sub>RhIn<sub>8</sub> will appear elsewhere [20].

The *P-T* phase diagram of Ce<sub>2</sub>RhIn<sub>8</sub> is shown in figure 7. At applied pressure,  $T_N$  is derived from the maximum of the temperature derivative of the resistivity  $\partial\rho(T)/\partial T$ . This definition of  $T_N$  is reasonable, as shown by a comparison to dc-susceptibility measurements carried out in a SQUID magnetometer for pressures up to 6 kbar.  $T_N$  decreases linearly at a rate  $\partial T_N/\partial P \approx -82$  mK/kbar. A linear extrapolation of these data to zero-temperature gives a critical pressure  $P_c \approx 30 \pm 5$  kbar. The initial slope and critical pressure of Ce<sub>2</sub>RhIn<sub>8</sub> are similar to those found for CeIn<sub>3</sub>,  $\partial T_N/\partial P \approx$

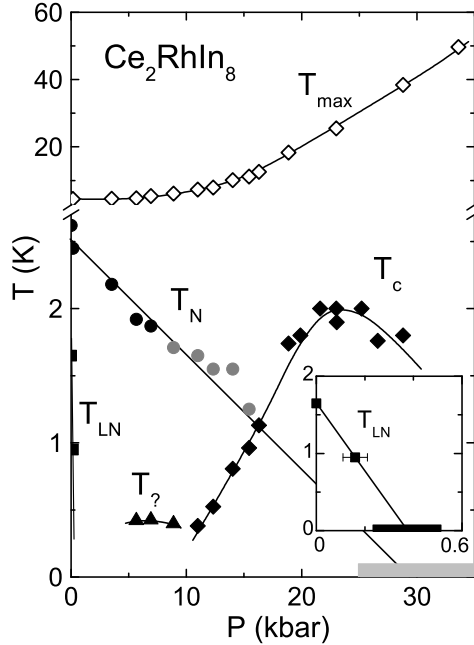


Fig. 7.  $P$ - $T$  phase diagram of  $\text{Ce}_2\text{RhIn}_8$  derived from resistivity measurements. The high temperature part shows the temperature of the maximum in the resistivity  $T_{\text{max}}$ . In the low temperature region  $T_N$  denotes the Néel transition and  $T_{\text{LN}}$  a second magnetic transition at low temperatures and small pressures (see inset). The superconducting temperature  $T_c$  is obtained from the onset onset of the resistive transition.  $T_?$  marks an additional feature of unknown origin in the resistivity.

–60 mK/kbar and 25 kbar, respectively [1]. These pressure dependencies contrast sharply with that of  $\text{CeRhIn}_5$  where  $T_N$  initially increases weakly with pressure [2,21].

In contrast to  $T_N$ , the incommensurate magnetic transition  $T_{\text{LN}}$  in  $\text{Ce}_2\text{RhIn}_8$  is very sensitive to external pressure as shown in the inset of Fig. 7. At 0.2 kbar  $T_{\text{LN}}$  shifts from 1.65 K at ambient pressure to 0.95 K. This gives an estimate of a critical pressure  $P_{c,\text{LN}} \approx (0.4 \pm 0.1)$  kbar for suppressing  $T_{\text{LN}}$  and a corresponding slope of  $\partial T_{\text{LN}}/\partial P \approx -(4.3 \pm 1.5)$  K/kbar.

Between 5.5 and 8.9 kbar a weak decrease in the resistivity appears at  $T_? = 420$  mK. We note that the maximum in the resistivity at  $T_{\text{max}}$  begins to increase when  $T_?$  first appears (see Fig. 7). We have no evidence for the nature of this feature in the resistivity, but one could speculate that it might be related to the suppression of the lower magnetic transition at  $P_{c,\text{LN}} \approx 0.4$  kbar.

At 11.0 kbar the resistivity data develop a steeper slope below  $\sim 1$  K followed by a kink near  $T_c = 380$  mK. The kink shifts continuously to

higher temperatures with increasing pressure, accompanied by a dramatically reduced resistivity at the experimental base temperature and finally a zero-resistance state appears below 595 mK at 16.3 kbar. Ac-susceptibility measurements show the onset of a diamagnetic response at the same temperature where the resistance goes to zero.  $T_c$  defined by the onset of the resistive transition shows a maximum at about 23 kbar. The extrapolated critical pressure for the suppression  $T_N$  is centered below the maximum  $T_c$  in the superconducting dome, similar to CeIn<sub>3</sub> [1]. The possible coexistence of antiferromagnetism and superconductivity promotes the importance of spin-fluctuations for the emergence of superconductivity in Ce<sub>2</sub>RhIn<sub>8</sub>.

### 3. Conclusions

It is generally believed that spin fluctuations mediate pairing in the unconventional superconductivity of heavy-fermion materials [1]. Both, the doping series CeRh<sub>1-x</sub>Ir<sub>x</sub>In<sub>5</sub> and Ce<sub>2</sub>RhIn<sub>8</sub> show the coexistence of superconductivity and antiferromagnetism in their phase diagrams. In Ce<sub>2</sub>RhIn<sub>8</sub> superconductivity appears with the suppression of its commensurate antiferromagnetic phase with applied pressure. The same is true for the parent compound CeIn<sub>3</sub> [1]. CeRhIn<sub>5</sub> orders in an incommensurate magnetic structure with  $Q = (\frac{1}{2}, \frac{1}{2}, 0.297)$  and  $\mu_0 = 0.37\mu_B$  [4]. Recent results of neutron diffraction measurements on CeRhIn<sub>5</sub> at 11 kbar show an abrupt change in the magnetic modulation corresponding to a change in the turn angle of the spiral structure from 107° to 142.6° [22] with little change in  $T_N$ . This suggests that the ordering wavevector tends to a commensurate magnetic structure with increasing pressure and leads to the speculation that superconductivity in CeRhIn<sub>5</sub> may evolve from a commensurate magnetic structure. However, this remains to be established. In this regard, though, we note that neutron diffraction experiments [23] on CeRh<sub>1-x</sub>Ir<sub>x</sub>In<sub>5</sub> find a commensurate magnetic structure developing at temperatures slightly below the incommensurate phase transition for values of  $x$  where superconductivity and antiferromagnetism coexist. (The transition between incommensurate and commensurate structures is not detectable by specific heat or resistivity measurements.) This leads us to speculate that the rapid suppression of the magnetic phase boundary  $x_c$  with pressure may be associated with a change in electronic structure that supports the incommensurate magnetic structure.

Together, these findings suggest evidence for the relationship of a commensurate magnetic phase, the suppression of the magnetism to zero temperature and the appearance of superconductivity mediated by antiferromagnetic spin fluctuations.

Work at Los Alamos was performed under the auspices of the US DOE.

## REFERENCES

- [1] N.D. Mathur *et al.*, *Nature* **394**, 39 (1998); G. Knebel *et al.*, *Phys. Rev.* **B65**, 024425 (2001).
- [2] H. Hegger *et al.*, *Phys. Rev. Lett.* **84**, 4986 (2000).
- [3] A. Malinowski *et al.*, unpublished.
- [4] W. Bao *et al.*, *Phys. Rev.* **B62**, 14621(R) (2000); W. Bao *et al.*, *Phys. Rev.* **B63**, 219901(E) (2001).
- [5] W. Bao *et al.*, *Phys. Rev.* **B64**, 020401(R) (2001).
- [6] P. G. Pagliuso *et al.*, *Phys. Rev.* **B64**, 100503(R) (2001).
- [7] C. Petrovic *et al.*, *Europhys. Lett.* **53**, 354 (2001).
- [8] R. Movshovich *et al.*, *Phys. Rev. Lett.* **86**, 5152 (2001).
- [9] A. Bianchi *et al.*, *Phys. Rev.* **B64**, 220504(R) (2001).
- [10] E. G. Moshopoulou *et al.*, *J. Solid State Chem.* **158**, 25 (2001).
- [11] High-resolution measurements of the ac-susceptibility show the onset of screening currents below the onset of the resistive transition in CeIrIn<sub>5</sub>. P. Gegenwart *et al.*, unpublished.
- [12] M. Nicklas *et al.*, *J. Phys.: Condens. Matter* **13** L905 (2001).
- [13] W. Bao *et al.*, *Phys. Rev.* **B65**, 100505 (2002).
- [14] J.D. Thompson, J.M. Lawrence, in: *Handbook on the Physics and Chemistry of Rare Earths and Actinides* K.A. Gschneidner *et al.* (ed) vol. **19**, North-Holland, Amsterdam, 1994, p. 385.
- [15] H. Shishido *et al.*, *J. Phys. Soc. Jpn* **71**, 162 (2002).
- [16] V. A. Sidorov *et al.*, cond-mat/0202251.
- [17] G. -q. Zheng *et al.*, private communication.
- [18] M. Nicklas *et al.*, unpublished.
- [19] W. Bao *et al.*, unpublished.
- [20] M. Nicklas *et al.*, cond-mat/0204064.
- [21] T. Muramatsu *et al.*, *J. Phys. Soc. Jpn* **70**, 3362 (2001).
- [22] S. Majumdar *et al.*, cond-mat/0205667.
- [23] A. D. Christianson *et al.*, unpublished.